

# Understanding global teleconnections of climate to regional model estimates of Amazon ecosystem carbon fluxes

CHRISTOPHER POTTER\*, STEVEN KLOOSTER†, MICHAEL STEINBACH‡, PANG-NING TAN‡, VIPIN KUMAR‡, SHASHI SHEKHAR‡ and CLAUDIO REIS DE CARVALHO§

\*NASA Ames Research Center, Moffett Field, CA, USA, †California State University Monterey Bay, Seaside, CA, USA,

‡University of Minnesota, Minneapolis, MN, USA, §Embrapa Amazônia Oriental, Belém – Pará, Brazil

## Abstract

We have investigated global teleconnections of climate to regional satellite-driven observations for prediction of Amazon ecosystem production, in the form of monthly estimates of net carbon exchange over the period 1982–1998 from the NASA–CASA (Carnegie–Ames–Stanford) biosphere model. This model is driven by observed surface climate and monthly estimates of vegetation leaf area index (LAI) and fraction of absorbed PAR (fraction of photosynthetically active radiation, FPAR) generated from the NOAA satellite advanced very high-resolution radiometer (AVHRR) and similar sensors. Land surface AVHRR data processing using modified moderate-resolution imaging spectroradiometer radiative transfer algorithms includes improved calibration for intra- and intersensor variations, partial atmospheric correction for gaseous absorption and scattering, and correction for stratospheric aerosol effects associated with volcanic eruptions. Results from our analysis suggest that anomalies of net primary production and net ecosystem production predicted from the NASA–CASA model over large areas of the Amazon region east of 60°W longitude are strongly correlated with the Southern Oscillation index. Extensive areas of the south-central Amazon show strong linkages of the FPAR and the NASA–CASA anomaly record to the Arctic Oscillation index, which help confirm a strong relation to southern Atlantic climate anomalies, with associated impacts on Amazon rainfall patterns. Processes are investigated for these teleconnections of global climate to Amazon ecosystem carbon fluxes and regional land surface climate.

*Keywords:* carbon flux, ecosystem model, global climate, remote sensing

*Received 27 October 2002; revised version received 1 July 2003 and accepted 11 July 2003*

## Introduction

The Amazon region includes the largest remaining tropical forest ecosystem on Earth. The Amazon rain forest accounts for about 10% of the world's terrestrial productivity and vegetation biomass, and can play an important role in regulating the Earth's carbon cycle and climate (Cox *et al.*, 2000). Despite the Amazon's potential importance for climate regulation, the precise pattern of terrestrial sources and sinks for CO<sub>2</sub> and

other 'greenhouse gas' compounds remain uncertain for the region. These large gaps in our knowledge still exist to a great degree because many impacts of land cover and geochemical controls related to surface climatology have not been understood in adequate detail to determine precise regional flux controls for biogenic trace gases.

In recognition of the changing environmental conditions in the Amazon basin, international collaboration between scientists from Brazil, the United States, and the European Union have led to the 'Large Scale Atmospheric Biosphere Experiment in Amazonia' (or LBA) (see <http://lba.cptec.inpe.br/lba/eng/science.htm>). The LBA has been designed to address a number of the major science questions that emerge from rapid

Correspondence: C. Potter, Ecosystem Science and Technology Branch, NASA Ames Research Center, Mail Stop 242-4, Moffett Field, CA 94035, USA, tel. + 650 604 6164, fax + 650 604 4680, e-mail: cpotter@mail.arc.nasa.gov

changes in land cover over the region. One primary goal of LBA is to understand the regulators of carbon exchange and energy balance in all Amazon ecosystems (LBA, 1996). A chief emphasis is to up-scale measurements to the region by integrating flux field measurements, process model predictions, and land surface characterizations derived from remote sensing. Within this integrated study context, it is important to understand the natural variability occurring within the Amazon region, particularly with respect to large-scale ocean–atmosphere–biosphere connections.

The influence of ocean surface patterns, such as those associated with the El Niño–Southern Oscillation (ENSO), have been noted as significant global teleconnections for atmospheric circulation and land surface climate (Glantz *et al.*, 1991). Teleconnection is a term used in climatological studies to describe near-simultaneous variation in climate and related processes over widely separated points on earth. There are different phases in climate phenomenon such as the ENSO, which is called El Niño in the warm phase and La Niña in the cold phase. ENSO warming at the sea surface, which related to ocean–atmosphere heat exchange, typically extends to about 30°N and 30°S latitude, with lags into continental land areas of several months.

Several previous studies have attempted to document the influence ENSO events on the net primary production (NPP) and annual carbon balance of Amazon forest ecosystems (Prentice & Lloyd, 1998; Tian *et al.*, 1998; Potter *et al.*, 2001; Foley *et al.*, 2002). However, large-scale teleconnections between multiple climate indices and Amazon regional carbon fluxes have yet to be demonstrated, and may escape ready detection without the aid of spatial–temporal analysis tools designed specifically to uncover such associations, both weak and strong, between time series of climate index anomalies and spatially explicit estimates of carbon fluxes on the land. We also note that in a recent study applying principal component analysis to the Amazon climate data, Botta *et al.* (2002) showed that ENSO cycles explain only about 21% of the total variance in annual mean precipitation and temperature for the Amazon region. This implies that other global climate forces may be operating to drive ecosystem carbon cycling over substantial portions of the Amazon basin.

We report here on studies to identify and quantify teleconnections of ocean–atmosphere climate indices and terrestrial carbon fluxes for the Amazon region, as represented by monthly NPP and net ecosystem production (NEP) predicted using an ecosystem modeling approach that covers the period 1982–1998. A simulation model for NEP was used to generate these

regional carbon fluxes, because the number of ground-based measurements of Amazon NEP and NPP is highly limited in space and time. Our specific objectives are to (1) use satellite observations to make assessments of seasonal and interannual vegetation dynamics in the Amazon during the 1980s and 1990s, in relation to major climate indices, and (2) understand the major teleconnections of climate to carbon cycling patterns and processes in the Amazon region, using EOS satellite data products to drive a model of NEP. To interpret our results, it is also necessary to integrate information on when and where anomalies in NPP and NEP controllers (land surface temperature and precipitation) are linked to similar patterns in the climate indices.

### Global data and models

Several climate indices are of prime interest in this study of land teleconnections (Trenberth & Hurrell, 1994). We focus here primarily on the Southern Oscillation index (SOI) and the Arctic Oscillation (AO) index, and secondarily on two NINO indices. Correlations between these climate index anomalies and monthly gridded sea surface temperature (SST) (Bottomley *et al.*, 1990; Reynolds *et al.*, 2002) for 1982–1998 indicate the central areas of the ocean temperature record that can be most closely associated with each of the indices (Fig. 1). SOI is an indicator of atmospheric impacts of ENSO, computed as the standardized difference between sea level pressure (SLP) measured

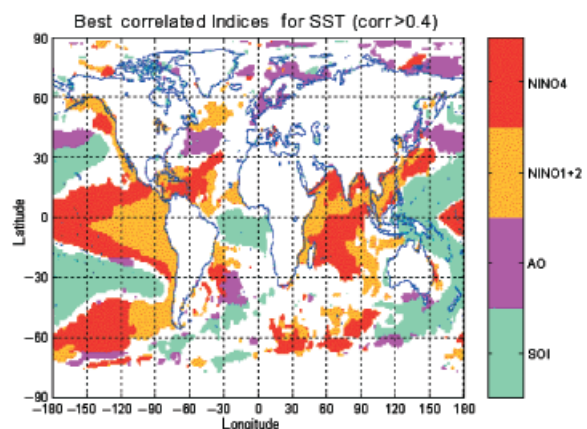


**Fig. 1** Areas of SST represented by correlation values of  $r > 0.4$  (Pearson's coefficient) in association with the SOI, AO, NINO1+2, and NINO4 indices for the period 1982–1998. Each non-white pixel indicates a pixel location where the SST record shows a significant correlation with at least one of the climate indices, and the color of that pixel indicates which of the indices has the highest correlation. Over 65% of global non-ice sea coverage is represented by the four-color coverage.

in Tahiti (17°S, 149°W) and Darwin, Australia (13°S, 131°E). The AO is derived from 1000 mb height anomalies poleward of 20°N (Thompson & Wallace, 1998). The NINO1 + 2 index is used to monitor SST over the eastern tropical Pacific, delineated by the area between 0°S–10°S and 90°W–80°W. The NINO4 index is used to monitor SST over the area between 5°N–5°S and 160°E–150°W. Although the SOI is the most commonly used of ENSO indicators, it is sometimes a poor predictor of La Niña (cold phase) events, compared with the NINO indices. Hence, it is necessary to use several ENSO indicators to capture its global impacts.

The SOI and NINO indices are commonly used to document warm-phases in ENSO, which are often associated with above-average temperatures in the northwestern half of the North American continent, and below-average temperatures in the southeastern half (Trenberth & Hurrell, 1994; Klein *et al.*, 1999; McCabe & Dettinger, 1999). There is also a pattern of the warm-phase ENSO associated with above-average precipitation over western coastal South America (Vuille *et al.*, 2000), the southern US, and northern Mexico, plus below-average precipitation in south-central Africa, northeastern South America, parts of southern Asia and Australia, and in North America from the Canadian Rockies to the Great Lakes region.

The AO is closely related to the North Atlantic Oscillation (NAO – measured between the Icelandic low (65°N, 22°W) and the Azores high pressure centers from 39°N, 9°W to 36°N, 6°W; Walker & Bliss, 1932), which, in its 'high index' warm phase can represent the persistence of above-average temperatures over North America and Europe, and below-average temperatures variations over North Africa and the Middle East. During winters when the AO index is high, anomalously low precipitation commonly occurs over the Canadian Arctic, central and southern Europe, the Mediterranean and Middle East. In contrast, anomalously high precipitation occurs from Iceland though Scandinavia (Hurrell, 1995).

For this analysis with climate index teleconnections, terrestrial NPP and NEP fluxes have been computed monthly (over the period 1982–1998) at a spatial resolution of 0.5° latitude–longitude using the NASA-CASA (Carnegie–Ames–Stanford) biosphere model (Potter, 1999; Potter *et al.*, 1999). NASA-CASA is a numerical model of monthly fluxes of water, carbon, and nitrogen in terrestrial ecosystems. Our estimates of terrestrial NPP fluxes depend on inputs of global satellite observations for land surface properties and on gridded model drivers from interpolated weather station records (New *et al.*, 2000) distributed across all the continental masses. Consequently, the NASA-CASA predictions of terrestrial NPP carbon fluxes are

derived with no dependence whatsoever on climate index data, nor on atmospheric circulation model predictions of surface climate patterns.

Our fundamental approach to estimate terrestrial NPP is to define optimal metabolic rates for carbon fixation processes, and to adjust these rate values using factors related to the limiting effects of time varying solar radiation, air temperature (TEMP), precipitation (PREC) (New *et al.*, 2000), predicted soil moisture, and land cover (DeFries & Townshend, 1994). Carbon (CO<sub>2</sub>) fixed by vegetation as NPP is estimated in the ecosystem model according to the time-varying (monthly mean) fraction of photosynthetically active radiation (FPAR) intercepted by plant canopies and a light utilization efficiency term (*emax*). This product is modified by stress factors for temperature (*Ta*) and moisture (*W*) that vary over time and space. The *emax* term is set uniformly at 0.39 gC (MJ<sup>-1</sup> PAR) (Potter *et al.*, 1993), a value that has been validated globally by comparing predicted annual NPP to more than 1900 field estimates of NPP (Fig. 2). In separate studies, interannual NPP fluxes from the CASA model were reported (Behrenfeld *et al.*, 2001) and validated against

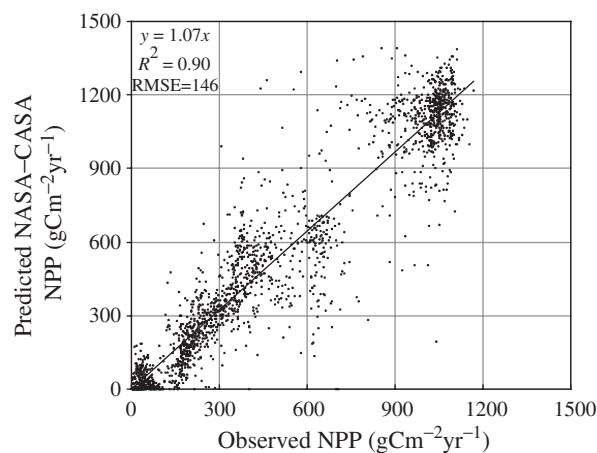


**Fig. 2** Comparison of annual observed NPP to predicted values from the NASA-CASA model (driven by 0.5° FPAR from the satellite AVHRR and climate means from New *et al.*, 2000). The data set of more than 1900 observed NPP points was compiled for the Ecosystem Model-Data Intercomparison (EMDI) activity by the Global Primary Productivity Data Initiative (GPPDI) working groups of the International Geosphere Biosphere Program Data and Information System (IGBP-DIS). Analysis of the residuals of this regression shows that scatter around the least squares regression line is due as much to uncertainties in scaling and inconsistencies in the ground-based measurements of NPP reported in sub-tropical ecosystems as to the prediction uncertainties represented in the NASA-CASA model. A more complete analysis of the residuals is presented in Potter *et al.* (2003).

multi-year estimates of NPP from field stations and tree rings (Malmström *et al.*, 1997).

Our NASA-CASA model is designed to couple seasonal patterns of NPP to soil heterotrophic respiration ( $R_h$ ) of  $\text{CO}_2$  from soils worldwide (Potter, 1999). First-order decay equations simulate exchanges of decomposing plant residue (metabolic and structural fractions) at the soil surface. The model also simulates surface soil organic matter (SOM) fractions that presumably vary in age and chemical composition. Turnover of active (microbial biomass and labile substrates), slow (chemically protected), and passive (physically protected) fractions of the SOM are represented. NEP can be computed as NPP minus total  $R_h$  fluxes, excluding the effects of small-scale fires and other localized disturbances or vegetation regrowth patterns on carbon fluxes (Schimel *et al.*, 2001).

Whereas previous versions of the NASA-CASA model (Potter *et al.*, 1993, 1999) used a normalized difference vegetation index (NDVI) to estimate FPAR, the current model version instead relies upon canopy radiative transfer algorithms (Knyazikhin *et al.*, 1998), which are designed to generate improved spatially varying FPAR products as inputs to carbon flux calculations. These radiative transfer algorithms, developed for the MODIS (moderate resolution imaging spectroradiometer) aboard the NASA Terra platform, account for attenuation of direct and diffuse incident radiation by solving a three-dimensional formulation of the radiative transfer process in vegetation canopies. Monthly gridded composite data from spatially varying channels 1 and 2 of the advanced very high-resolution radiometer (AVHRR) have been processed according to the MODIS radiative transfer algorithms and aggregated over the global land surface to  $0.5^\circ$  grid resolution, consistent with the NASA-CASA model driver data for climate variables.

#### Land climate controls on ecosystem carbon fluxes

In this analysis, the Amazon region has been defined broadly as the South American land area between the northwestern corner of  $6^\circ\text{N}$ ,  $77^\circ\text{W}$  and the southeastern corner of  $20^\circ\text{S}$  and  $45^\circ\text{W}$ . Terrestrial NPP for this Amazon regional coverage was estimated by our NASA-CASA model to vary between 8.7 (in 1983) and 9.8  $\text{PgC yr}^{-1}$  (in 1997), with a seasonal anomaly range of about  $\pm 0.1 \text{ PgC month}^{-1}$  (Fig. 3a). The model predicts a general increase in NPP for the region over this 17-year time period of 1982–1998.

The regional predicted NEP flux for atmospheric  $\text{CO}_2$  varied between an annual source (to the atmosphere) of  $-0.17 \text{ PgC yr}^{-1}$  in 1983 to a sink (from the atmosphere) of  $+0.64 \text{ PgC yr}^{-1}$  in 1989, with a seasonal anomaly

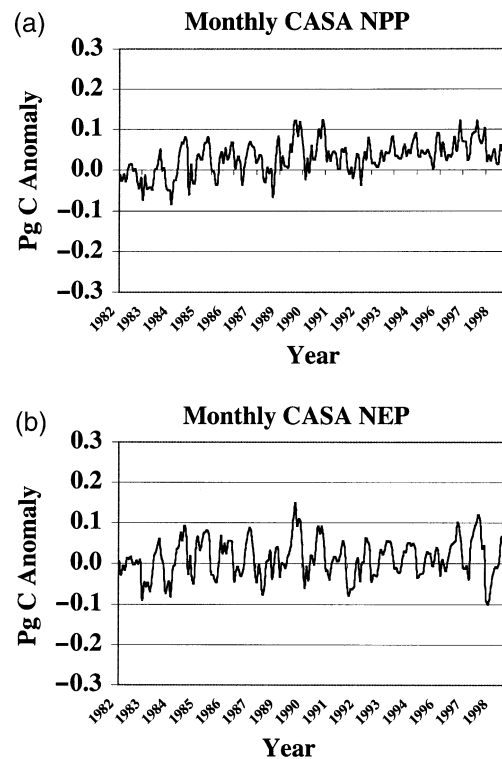
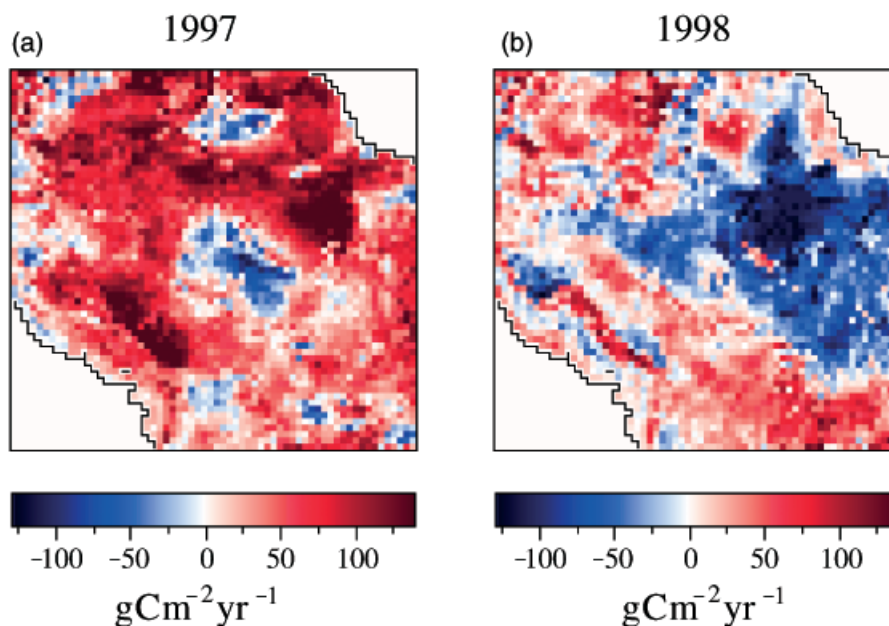


Fig. 3 Regionally summed carbon fluxes from the NASA-CASA model as monthly anomalies from pre-1982 climate results for Amazon (a) NPP and (b) NEP.

range of up to  $\pm 0.1 \text{ PgC month}^{-1}$  (Fig. 3b). Our NASA-CASA model results are consistent with the findings of McGuire *et al.* (2001) and Vukicevic *et al.* (2001) that in the tropical zones there is a net release of carbon to the atmosphere during El Niño years, and a net uptake during non El Niño years. This model result is illustrated in the comparison between annual NEP fluxes for 1997 and 1998 for the Amazon region (Fig. 4), the years that bounded the last major El Niño event of the century. For the relatively wet periods during 1997, predicted annual NEP flux was a net sink of  $0.55 \text{ PgC}$ . For the El Niño event that started in late 1997, predicted annual NEP flux in 1998 was  $-0.03 \text{ PgC}$ , mainly because of the conversion of carbon sinks to sources in the eastern portions of the basin.

Several previous studies of ecosystem modeling, namely, Kindermann *et al.* (1996), Tian *et al.* (1998), Prentice & Lloyd (1998), Asner *et al.* (2000), Potter *et al.* (2001), and Foley *et al.* (2002), have examined how interannual variations in climate affect the carbon balance of the Amazon basin. As in the present study, all of these models suggest that the net annual flux of carbon by the basin is significantly correlated to ENSO events. The Amazon basin is predicted to be a significant carbon sink during La Niña events, and a



**Fig. 4** Predicted annual NEP from the NASA–CASA model for the Amazon region in 1997 and 1998. Positive values (red) represent net sink fluxes of atmospheric CO<sub>2</sub> into terrestrial ecosystems, where negative values (blue) represent net source fluxes of atmospheric CO<sub>2</sub> from terrestrial ecosystems.

carbon source during El Niño events. Moreover, most of these modeling studies conclude that major variations in the regional carbon balance are related chiefly to changes in precipitation. The average El Niño event is drier than normal, and the average La Niña period is wetter in northern Amazonia. In southern Amazonia, both El Niño and La Niña periods are drier than neutral conditions.

Association rule analysis can offer further insights into the types of dependencies that exist among variables within a large model data set (Goodman & Kruskal, 1954). Non-random associations between two or more NASA–CASA model variables are reported here using the  $\chi^2$ -test (Stockburger, 1998).  $\chi^2$ -values greater than 3.84 (degrees of freedom = 1) indicate a high probability ( $P < 0.05$ ) of non-random association between anomalously low (LO) or anomalously high (HI) monthly events for TEMP or PREC with either NPP or NEP. We used an anomalous event threshold value of 1.5 standard deviations or greater from the long-term (1982–1998) monthly mean value. For our analysis, association patterns are reported below on the basis of frequency of occurrence within major global vegetation types (DeFries & Townshend, 1994).

The main result from this analysis is that below average PREC and above average TEMP can decrease predicted NPP and NEP in the Amazon region and in tropical ecosystems generally. Specifically, we find that one of the strongest non-random associations in our NASA–CASA results is that PREC-LO events co-occur

with NPP-LO and with NEP-LO events in evergreen broadleaf forests, deciduous broadleaf forests, croplands, and grassland savannas (Fig. 5). These events occur mainly in drought-sensitive areas of tropical and sub-tropical zones, and possibly in areas of major wild fires that are associated with FPAR-LO events. We also find that TEMP-HI events co-occur with NPP-LO events for these same vegetation types, which can be another indicator of drought stress effects on plant carbon gains. It is possible, nevertheless, that the inferred TEMP-HI association with NPP-LO could be the result of statistical co-variation between high temperature and low precipitation across the region.

We also examined the associations between positive or negative anomalies in TEMP and anomalies in predicted  $R_h$  fluxes of CO<sub>2</sub> from soils. Results suggest that above-average TEMP anomalies can lead to a decrease in predicted  $R_h$  over the Amazon region and in moist tropical ecosystems generally. This association is most prominent in the northeastern section of the Amazon basin region (map results not shown). We hypothesize that decreases in soil moisture with higher TEMP conditions are responsible for this association with a decrease in predicted  $R_h$  fluxes.

#### Time series teleconnections

As a first step in analysis of global teleconnections, we examined the underlying empirical relationships between land climate records, those used as input to the

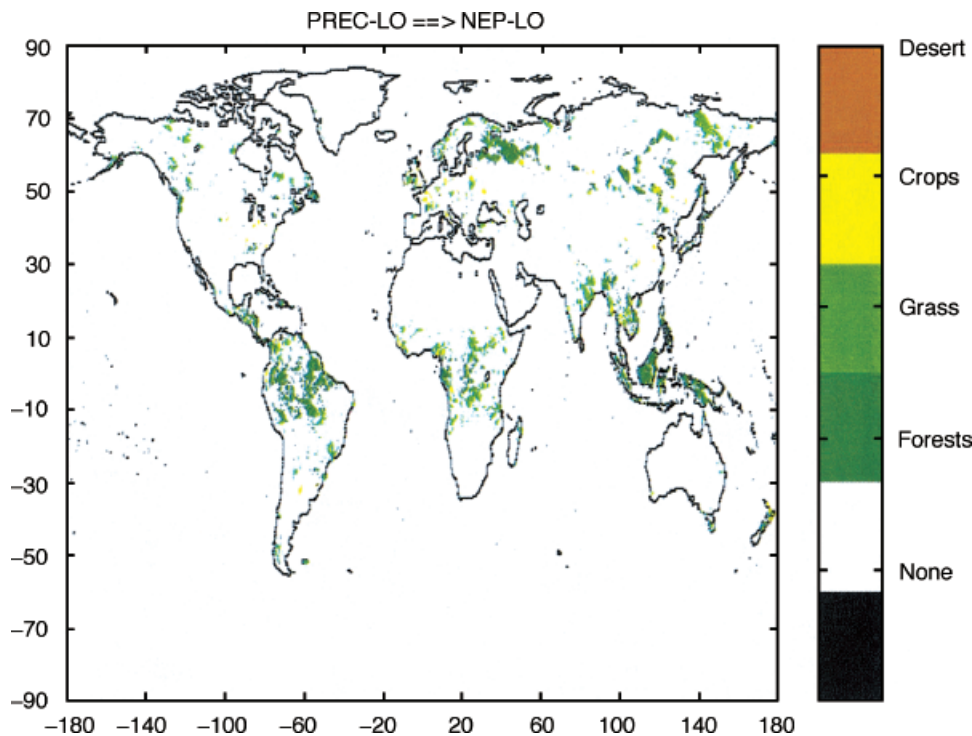


**Fig. 5** Locations of co-occurrence between anomalously low (LO) monthly PREC and NASA-CASA predicted NEP from 1982 to 1998. An anomalous event threshold value was defined as 1.5 standard deviations or greater from the long-term (1982–1998) monthly mean value. Each non-white pixel indicates a location where NEP-LO co-occurs in the time series with PREC-LO and that the color of that pixel indicates the vegetation type at that location.

NASA-CASA model, and the selected climate indices. We address the questions of where and how are land surface temperature and precipitation time series used as model input variables correlated with ENSO and AO. Our analysis here covers a long-term (1958–1998) historical record to assess the impacts of ENSO and AO on the Amazon region, rather than concentrating on individual ENSO events of the past 20 years. By considering several decades of climate cycles, we can more accurately assess the impacts of climate events on the Amazon basin, and their statistical significance.

Serial correlation (i.e., autocorrelation) needs to be considered when testing significance of the association between two time series. We have determined the serial correlation of climate indices at all possible lag times up to 6 months. SOI anomalies have a low autocorrelation function ( $<0.3$ ) at lag times greater than about 6 months (using index data from 1958–1995). The same is true for the NINO1 + 2 index anomalies. For the NAO/AO anomalies, the autocorrelation function is  $<0.1$  at lag times greater than 3 months. For our predicted NPP anomalies, the autocorrelation function is  $<0.1$  at lag times greater than 6 months. Based on these results, we accepted degrees of freedom (d.f.) for the climate index time series correlations with NPP fluxes to be d.f. = 32 (34 ‘seasons’ of 6 months duration

in a 17-year window, minus 2 for a two-tailed test of significance). For the purposes of demonstrating a significant association with measured climate index values at d.f. = 32, Pearson’s correlation coefficient ( $r$ )  $>0.34$  carries a relatively high confidence level of  $P < 0.05$ . When dealing with long-term climate correlations and d.f.  $>75$  (for roughly 40 years of global records), values of  $r > 0.2$  carry the same confidence level of  $P < 0.05$ .

Like Mason & Goddard (2001) and Foley *et al.* (2002), we report on an analysis of the long-term climate data from the Climate Research Unit of the University of East Anglia, Norwich (New *et al.*, 2000; hereinafter referred to as the CRU05 dataset). CRU05 is a global, monthly mean data set of TEMP, PREC, humidity, and cloudiness at  $0.5^\circ$  by  $0.5^\circ$  latitude/longitude resolution, for the period 1901–1995. The climate record is most reliable after the 1940s; we therefore restricted our analysis to the 40-year period between 1958 and 1998.

Correlations between the time series anomalies of the SOI, AO, NINO1 + 2, and NINO4 climate indices and  $0.5^\circ$  PREC or TEMP on land were identified. The first step in this analysis was the conversion of all time series to Z-score values, which can be used to specify the relative statistical location of each monthly value within the 40-year population distribution. The numerical

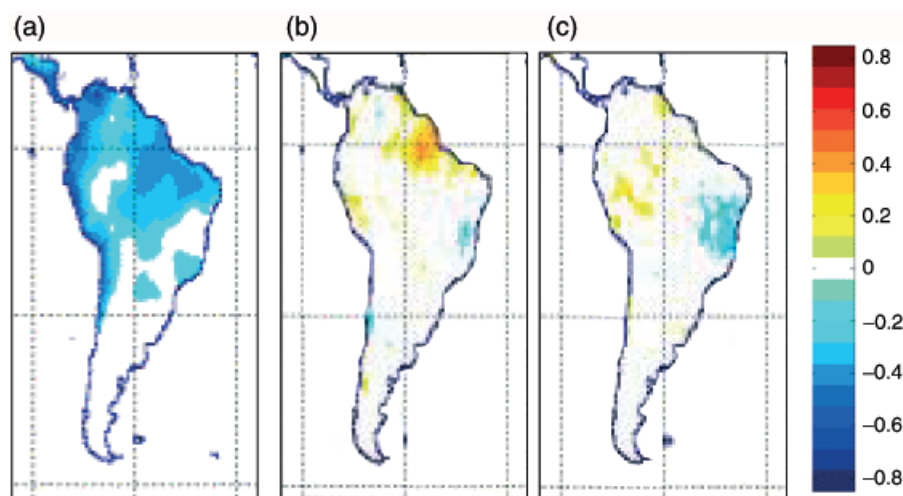


**Fig. 6** Regional extent of Pearson's coefficient for correlation  $r > 0.2$  of CRU5 climate with climate indices (1958–98) (a) TEMP with SOI, (b) PREC with SOI, and (c) PREC with AO.

Z-score indicates the distance from the 40-year mean as the number of standard deviations above or below the mean. The difference between the  $t$ -statistic and the Z-score is that the  $t$ -test uses a sample standard deviation, whereas the Z-score uses population standard deviation.

Results show that CRU5 land TEMP records for the period 1958–1998 were strongly correlated with SOI throughout the entire Amazon region, with the exception of the extreme western portions of the Brazilian Amazon mainly located between  $6^{\circ}\text{S}$  and  $14^{\circ}\text{S}$  (Fig. 6a). El Niño events are systematically warmer and La Niña events are systematically cooler in the Amazon region than neutral years in the SOI record. CRU5 land TEMP records were strongly correlated with NINO4 across the entire northern hemisphere portion of the Amazon land region (map not shown). The only areas showing strong correlation of TEMP with either NINO1 + 2 or AO were located in the extreme northeastern corner of the Amazon region (maps not shown).

On a regional basis, land PREC correlations with all four climate indices were generally strongest during the northern hemisphere winter (December–January–February, DJF) and autumn (September–October–November, SON) months, compared with the spring (March–April–May, MAM) and summer (June–July–August, JJA) months (Trenberth & Hurrell, 1994; Hurrell, 1995). Results show that CRU5 land DJF PREC records for the period 1958–1998 were most strongly correlated with SOI in the northeastern Amazon region between  $3^{\circ}\text{N}$  and  $7^{\circ}\text{S}$  (Fig. 6b). Our SOI correlation results are consistent with those of Halpert & Ropelewski (1992), Mason & Goddard (2001), Marengo *et al.* (2001), and Foley *et al.* (2002), who reported that the average El Niño is drier than neutral

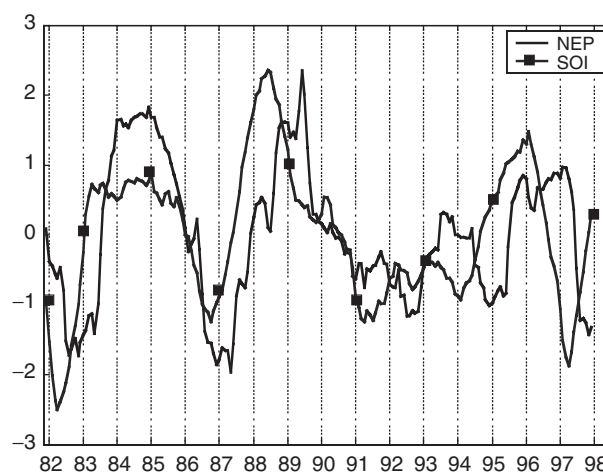


**Fig. 7** Time-series correlation of anomalies of 12-month running average SOI with predicted NEP at  $5^{\circ}\text{S}$ ,  $50^{\circ}\text{W}$ ,  $r = +0.79$ .

conditions in the Amazon region, while the average La Niña is wetter. CRU5 land PREC records were strongly correlated with both NINO1 + 2 and NINO4 indices in the northeastern corner of the Amazon region (maps not shown). The strongest DJF PREC correlations with AO were located in the extreme western and southeastern portions of the Amazon region (Fig. 6c).

Turning to carbon flux correlations, we used matching monthly records for the period of 1982–1998 to investigate associations between the time series anomalies of the climate indices and predicted carbon fluxes on land from the NASA–CASA model. The 12-month running mean was computed to deseasonalize the NASA–CASA model time series. An example of the close association between SOI and predicted land carbon fluxes is shown in Fig. 7 for a location in the eastern Amazon (at  $5^{\circ}\text{S}$ ,  $50^{\circ}\text{W}$ ), in Pará about 100 km

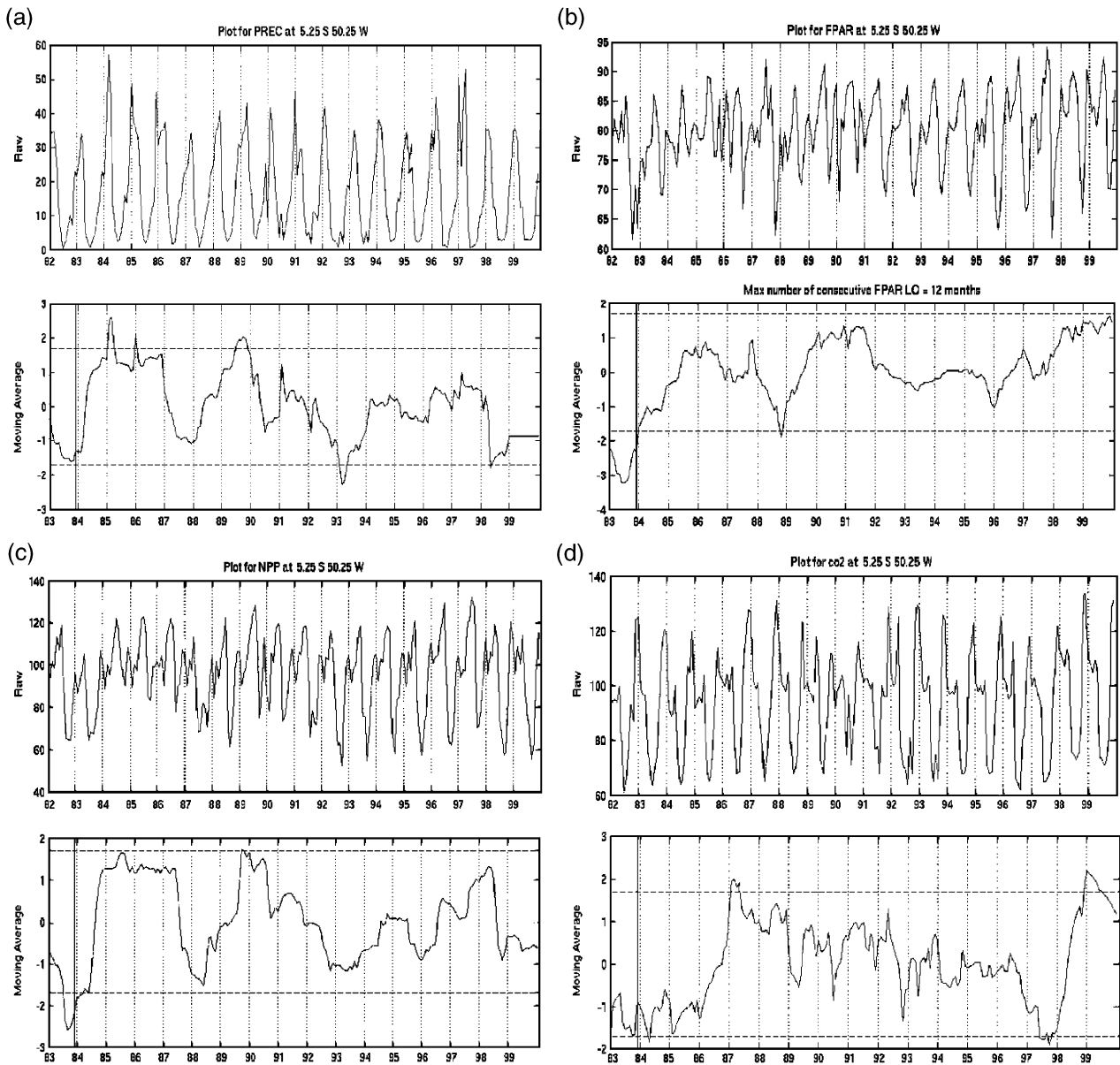


Fig. 8 Time-series of raw and 12-month running average (a) FPAR, (b) PREC, (c) predicted NPP carbon, and (d) predicted  $R_H$ -CO<sub>2</sub> at 5° S, 50° W.

northwest of the city of Marabá. Both the SOI and modeled carbon fluxes show low points in 1982–1983, 1986–1987, 1992, and 1997–1998, with an time series correlation of  $r = 0.79$  for SOI with NEP, and  $r = 0.85$  for the correlation of SOI with NPP ( $P < 0.05$ ). We find that a seasonal phase shift in climate index lead times of up to 6 months commonly improved correlations with the NPP and NEP time series anomalies. The 2–6 month lead between the climate indices and NEP results principally from phase differences between the climate indices and the model inputs (TEMP, PREC, and FPAR) used to generate NEP.

A marked similarity can be seen between the 12-month moving average PREC and predicted NPP for this location at 5° S, 50° W (Fig. 8), compared with the weaker relationship between the moving average FPAR and predicted NPP. This is most obvious in the periods after 1995, when FPAR steadily increases, while high interannual variability in PREC prevents NPP from following the same upward pattern as FPAR. Predicted  $R_H$  fluxes of CO<sub>2</sub> from soil at this location generally lag NPP responses to PREC by 1 or 2 years and are more variable from month to month or season to season within a year.

An example of the association between AO and predicted land carbon fluxes is shown in Fig. 9 for a location in the southern Amazon (at 15°S, 55°W), in Mato Grosso about 100 km northeast of the city of Cuiabá. The AO index and NEP fluxes both show rapid increases in 1985–1986 and 1988–1989, which can be attributed to increasing precipitation and temperature on land during these transition periods. We find a time series correlation at this location of  $r = 0.41$  ( $P < 0.05$ ) for AO with NEP and also with observed FPAR. The time series correlation for AO with NPP was slightly higher at  $r = 0.55$ .

Regional correlation maps (Fig. 10a–c) show the areas where  $r > 0.34$  for associations of the SOI, NINO1 + 2, and AO indices with our predicted NEP fluxes for the period 1982–1998. Seasonality in all time series records was removed before this analysis by computing a 12-month moving average. We find that deseasonalized NEP fluxes have strong correlations with SOI and NINO1 + 2 for 59% and 47%, of the Amazon regional area, respectively. Predicted NEP fluxes have strong

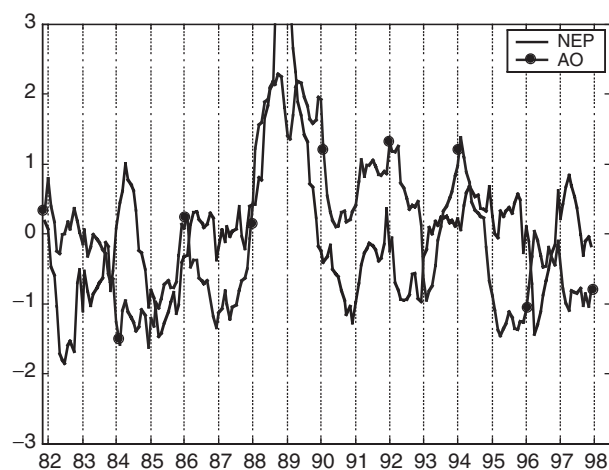


Fig. 9 Time-series correlation of anomalies of 12-month running average AO with predicted NEP at 15°S, 55°W,  $r = +0.41$ .

correlations with AO for 20% of the regional area. The AO regional correlation with predicted NEP has a completely different coverage pattern than the NEP correlation pattern with either SOI or NINO1 + 2, which are similar in many respects.

For deseasonalized NPP anomalies, 45% and 19% of the Amazon regional area have strong correlations with SOI and AO indices, respectively. In comparison to these NASA–CASA model outputs, the FPAR input time series of deseasonalized anomalies have strong correlations with SOI and AO over 25% and 17% of the Amazon regional area, respectively. This implies that climate (PREC and TEMP) together with FPAR inputs to the NASA–CASA model are strongly influencing carbon flux correlations with SOI, whereas FPAR alone accounts for the strongest carbon flux correlations with AO.

The relative impacts of PREC and TEMP time series inputs (to the NASA–CASA carbon model) on correlations between climate indices SOI and AO with our predicted NEP fluxes can be examined further by comparison of Figs 6 and 10. For example, we find that nearly 89% of total Amazon regional area shown in Fig. 10a as having strong correlation of NEP with SOI also shows strong correlation of TEMP with SOI (Fig. 6a). This includes practically all of the forested area in the eastern half of the region. In comparison, 24% of total Amazon regional area shown in Fig. 10a as having strong correlation of NEP with SOI also shows strong correlation of DJF PREC with SOI (Fig. 6b), which is composed mainly of the northeastern forest area of the region. We can conclude therefore that the strongest correlations of predicted NEP with SOI over the 17-year time series can be attributed to the combined effects of PREC and TEMP inputs to our ecosystem model, but that the effects of ENSO-related TEMP variations alone on predicted NEP cannot be overlooked, especially in the southeastern forest area of the region.

In contrast to NEP and SOI results, we find that just 6% of the total Amazon regional area shown in Fig. 10c

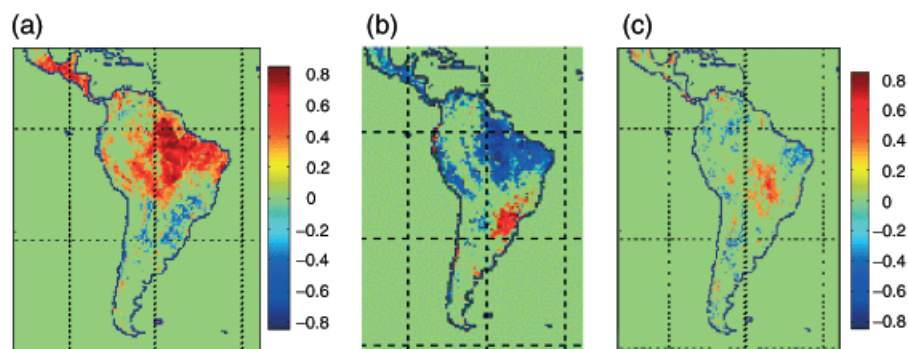


Fig. 10 Regional extent of Pearson's coefficient for correlation  $r > 0.34$  of predicted terrestrial NEP (1982–98) with (a) SOI, (b) NINO1 + 2, and (c) AO indices.

as having strong correlation of NEP with AO also shows strong correlation of DJF PREC with AO (Fig. 6c), while only 2% of total land area shown in Fig. 10c shows strong correlation of TEMP with AO (map not shown). Consequently, the great majority of the regional area shown in Fig. 10c as having strong NEP correlations with AO must result from FPAR inputs to the NASA–CASA carbon model, which also correlate strongly with AO over extensive areas of central and southern Brazil.

### Discussion and conclusions

Ecosystem modeling studies like those of Tian *et al.* (1998) and Foley *et al.* (2002) have implied that major variations in the regional carbon balance of the Amazon are related chiefly to ENSO precipitation patterns. While our study results are consistent with these previous findings, mainly for the northern portion of the Amazon region, this analysis suggests that temperature effects of ENSO cycles and AO-related climate events can also have notable impacts on Amazon carbon fluxes over decade-long time periods. Specifically, NASA–CASA model anomalies from 1982–1998 for NPP and NEP over large areas of the Amazon region east of 60°W longitude are strongly correlated with the SOI. As the means to explain NEP anomalies, reasonably strong TEMP correlations with SOI are more widespread regionally than are strong PREC correlations with SOI. It is worth noting that NASA–CASA has the potential to generate results that are different than the two other models cited above, because NASA–CASA relies on satellite data as an input. The AHVRR time series is an observation of the actual land vegetation dynamics, which is lacking in the two other cited models, and which can be sensitive to variability on temperature as well as precipitation.

The tropical inland areas of central and southern Brazil that show strong correlations for FPAR, NPP, and NEP with AO (Fig. 9c) are noteworthy, particularly because these patterns in the 17-year satellite record of measured FPAR patterns can corroborate the findings of atmospheric simulation studies that have recently implied a strong influence of southern Atlantic SST anomalies on the NAO, with concurrent impacts on southern Amazon rainfall patterns (Robertson *et al.*, 2000). Our results here are an additional indicator of circulation and heating patterns associated with the South American monsoon system (SAMS), which may exert an important influence on the boreal winter subtropical jet over eastern North America, possibly through changes Amazon rainfall and regional Hadley circulations (Nogués-Paegle *et al.*, 1998). Several previous studies have addressed tropical North Atlantic

variability, which directly impacts the intertropical convergence zone (ITCZ) (Enfield & Mayer, 1997; Saravanan & Chang, 2000), and by the NAO (Namias, 1972). Many new studies are needed to address such variability over the South Atlantic, and the combined associations of ENSO, NAO, and the Antarctic Oscillation (AAO) on storm tracks over central and southern Brazil.

Ecosystem model results that are presented in the context of teleconnections with global climate processes can aid in understanding the mechanisms for sink fluxes of CO<sub>2</sub> in the terrestrial biosphere. Uncertainties remain to a large degree because the heterogeneity of land cover and ecosystem exchange processes have not been measured and mapped in adequate detail to determine precise geographic differences in sink/source controls (USGCRP, 1999; Watson *et al.*, 2000). Nonetheless, by a continuous process of integration and evaluation of ecosystem model predictions with ground-based measurements of carbon fluxes and remote sensing, such as those ongoing within the LBA program, these uncertainties are being narrowed rapidly, and the role of Amazonia in global climate change can be elucidated.

### Acknowledgments

This work was supported by grants from NASA programs for Terrestrial Ecology and LBA-ECO, Intelligent Systems and Intelligent Data Understanding, and the NASA Earth Observing System (EOS) Interdisciplinary Science Program. Ranga Myneni provided remote sensing data products for this study.

### References

- Asner GP, Townsend AR, Braswell BH (2000) Satellite observation of El Niño effects on Amazon forest phenology and productivity. *Geophysical Research Letters*, **27**, 981–984.
- Behrenfeld MJ, Randerson JT, McClain CR *et al.* (2001) Biospheric primary production during an ENSO transition. *Science*, **291**, 2594–2597.
- Botta A, Ramankutty N, Foley JA (2002) Long-term variations of climate and carbon fluxes over the Amazon basin. *Geophysical Research Letters*, **29** DOI 10.1029/2001GL013607.
- Bottomley M, Folland CK, Hsiung J *et al.* (1990) Global ocean surface temperature atlas 'GOSTA' Meteorological Office, Bracknell, UK and the Department of Earth, Atmospheric and Planetary Sciences, Massachusetts Institute of Technology, Cambridge, MA, USA.
- Cox P, Betts R, Jones C *et al.* (2000) Acceleration of global warming due to carbon-cycle feedbacks in a coupled climate model. *Nature*, **408**, 184–187.
- DeFries R, Townshend J (1994) NDVI-derived land cover classification at global scales. *International Journal of Remote Sensing*, **15**, 3567–3586.
- Enfield DB, Mayer DA (1997) Tropical Atlantic sea surface temperature variability and its relation to El Niño–Southern Oscillation. *Journal of Geophysical Research*, **102**, 929–945.

- Foley JA, Botta A, Coe MT *et al.* (2002) The El Niño/Southern Oscillation and the climate, ecosystems and rivers of Amazonia. *Global Biogeochemical Cycles*, DOI 10.1029/2002GB001872.
- Goodman LA, Kruskal WH (1954) Measures of association for cross-classifications. *Journal of the American Statistical Association*, **49**, 732–764.
- Glantz MH, Katz RW, Nicholls N (eds) (1991) *Teleconnections Linking World-Wide Climate Anomalies*. Cambridge University Press, New York.
- Halpert MS, Ropelewski CF (1992) Surface-temperature patterns associated with the Southern Oscillation. *Journal of Climate*, **5**, 577–593.
- Hurrell JW (1995) Decadal trends in the North Atlantic Oscillation regional temperatures and precipitation. *Science*, **269**, 676–679.
- Kindermann J, Wurth G, Kohlmaier GH *et al.* (1996) Interannual variation of carbon exchange fluxes in terrestrial ecosystems. *Global Biogeochemical Cycles*, **10**, 737–755.
- Klein SA, Soden BJ, Lau N-C (1999) Remote sea surface temperature variations during ENSO: evidence for a tropical atmospheric bridge. *Journal of Climate*, **12**, 917–932.
- Knyazikhin Y, Martonchik JV, Myneni RB *et al.* (1998) Synergistic algorithm for estimating vegetation canopy leaf area index and fraction of absorbed photosynthetically active radiation from MODIS and MISR data. *Journal of Geophysical Research*, **103**, 32257–32276.
- LBA Science Planning Group (1996) *The Large Scale Biosphere–Atmosphere Experiment in Amazonia (LBA): Concise Experimental Plan*. Cachoeira Paulista, SP, Brazil.
- Malmström CM, Thompson MV, Juday GP *et al.* (1997) Interannual variation in global scale net primary production: testing model estimates. *Global Biogeochemical Cycles*, **11**, 367–392.
- Marengo JA, Liebmann B, Kousky VE *et al.* (2001) Onset and end of the rainy season in the Brazilian Amazon Basin. *Journal of Climate*, **14**, 833–852.
- Mason SJ, Goddard L (2001) Probabilistic precipitation anomalies associated with ENSO. *Bulletin of the American Meteorological Society*, **82**, 619–638.
- McCabe GJ, Dettinger MD (1999) Decadal variations in the strength of ENSO teleconnections with precipitation in the western United States. *International Journal of Climatology*, **19**, 1399–1410.
- McGuire AD, Sitch S, Clein JS *et al.* (2001) Carbon balance of the terrestrial biosphere in the twentieth century: analyses of CO<sub>2</sub>, climate and land-use effects with four process-based ecosystem models. *Global Biogeochemical Cycles*, **15**, 183–206.
- Namias J (1972) Influence of northern hemisphere general circulation on drought in northeastern Brazil. *Tellus*, **24**, 336–342.
- New M, Hulme M, Jones P (2000) Representing twentieth century space-time climate variability. II. Development of 1901–1996 monthly grids of terrestrial surface climate. *Journal of Climate*, **13**, 2217–2238.
- Nogués-Paegle J, Mo K-C, Paegle J (1998) Predictability of the NCEP-NCAR reanalysis model during austral summer. *Monthly Weather Review*, **126**, 3135–3152.
- Potter CS (1999) Terrestrial biomass and the effects of deforestation on the global carbon cycle. *Bioscience*, **49**, 769–778.
- Potter C, Klooster S, Steinbach M *et al.* (2003) Global teleconnections of climate to terrestrial carbon flux. *Journal of Geophysical Research*, DOI 10.1029/2002JD002979.
- Potter CS, Klooster S, de Carvalho CR *et al.* (2001) Modeling seasonal and interannual variability in ecosystem carbon cycling for the Brazilian Amazon region. *Journal of Geophysical Research*, **106**, 10423–10446.
- Potter CS, Brooks-Genovese V, Klooster SA *et al.* (2001) Biomass burning losses of carbon estimated from ecosystem modeling and satellite data analysis for the Brazilian Amazon region. *Atmospheric Environment*, **35**, 1773–1781.
- Potter CS, Klooster SA, Brooks V (1999) Interannual variability in terrestrial net primary production: exploration of trends and controls on regional to global scales. *Ecosystems*, **2**, 36–48.
- Potter CS, Randerson JT, Field CB *et al.* (1993) Terrestrial ecosystem production: a process model based on global satellite and surface data. *Global Biogeochemical Cycles*, **7**, 811–841.
- Prentice IC, Lloyd J (1998) C-quest in the Amazon basin. *Nature*, **396**, 619–620.
- Reynolds RW, Rayner NA, Smith TM *et al.* (2002) An improved *in situ* and satellite SST analysis. *Journal of Climate*, **15**, 1609–1625.
- Robertson AW, Mechoso CR, Kim Y-J (2000) The influence of Atlantic sea surface temperature anomalies on the North Atlantic Oscillation. *Journal of Climate*, **13**, 122–138.
- Saravanan R, Chang P (2000) Interactions between tropical Atlantic variability and El Niño–Southern Oscillation. *Journal of Climate*, **13**, 2177–2194.
- Schimel D, House J, Hibbard K *et al.* (2001) Recent patterns and mechanisms of carbon exchange by terrestrial ecosystems. *Nature*, **414**, 169–172.
- Stockburger DW (1998) *Introductory Statistics: Concepts, Models, And Applications*, WWW Version 1.0, <http://www.psychstat.smsu.edu/sbk00.htm>.
- Thompson DWJ, Wallace JM (1998) The Arctic Oscillation signature in the wintertime geopotential height and temperature fields. *Geophysical Research Letters*, **25**, 1297–1300.
- Tian HQ, Melillo JM, Kicklighter DW *et al.* (1998) Effect of interannual climate variability on carbon storage in Amazonian ecosystems. *Nature*, **396**, 664–667.
- Trenberth KE, Hurrell JW (1994) Decadal atmosphere–ocean variations in the Pacific. *Climate Dynamics*, **9**, 303–319.
- USGCRP (1999) A US carbon cycle science plan. In: *Report of the Carbon and Climate Working Group, US Global Change Research Program* (eds Sarmiento JL, Wofsy SC). Agencies of the United States Global Change Research Program, Washington DC, USA.
- Vuille M, Bradley RS, Keimig F (2000) Climate variability in the Andes of Ecuador and its relation to tropical Pacific and Atlantic sea surface temperature anomalies. *Journal of Climate*, **13**, 2520–2535.
- Vukicevic T, Braswell BH, Schimel D (2001) Diagnostic study of temperature controls on global terrestrial carbon exchange. *Tellus*, **53B**, 150–170.
- Walker GT, Bliss EW (1932) *World Weather V. Memoirs of Royal Meteorological Society*, **4**, 53–84.
- Watson RT, Noble IR, Bolin B *et al.* (eds) (2000) *Land Use, Land-Use Change, and Forestry Special Report of the Intergovernmental Panel on Climate Change*. Cambridge University Press, Cambridge, UK.